Impressed current cathodic protection of chloride-contaminated RC structures with cracking

A numerical study

Guo, Bingbing; Qiao, Guofu; Li, Zhenming; Li, Dongsheng; Dai, Jinghui; Wang, Yan

DOI
10.1016/j.jobe.2021.102943

Publication date
2021

Document Version
Final published version

Published in
Journal of Building Engineering

Citation (APA)
Guo, B., Qiao, G., Li, Z., Li, D., Dai, J., & Wang, Y. (2021). Impressed current cathodic protection of chloride-contaminated RC structures with cracking: A numerical study. *Journal of Building Engineering*, *44*, Article 102943. https://doi.org/10.1016/j.jobe.2021.102943

Journal of Building Engineering 44 (2021) 102943

Contents lists available at ScienceDirect

Journal of Building Engineering

journal homepage: http://www.elsevier.com/locate/jobe

Impressed current cathodic protection of chloride-contaminated RC structures with cracking: A numerical study

Bingbing Guo [a], Guofu Qiao [b], Zhenming Li [c, *], Dongsheng Li [d], Jinghui Dai [e], Yan Wang [a, **]

[a] National Key Laboratory of Green Building in West China / School of Civil Engineering / Key Lab of Engineering Structural Safety and Durability, Xi'an University of Architecture and Technology, Xi'an, 710055, China
[b] School of Civil Engineering, Harbin Institute of Technology, Harbin, 150090, China
[c] Department of Materials and Environment, Faculty of Civil Engineering and Geoscience, Delft University of Technology, Delft 2628 CN, the Netherlands
[d] School of Civil Engineering, Dalian University of Technology, Dalian, 116024, China
[e] School of Energy and Civil Engineering, Harbin University of Commerce, Harbin, 150028, China

ARTICLE INFO

Keywords:
Impressed current cathodic protection
Reinforced concrete structures
Cracks
Steel corrosion
Numerical modelling

ABSTRACT

Impressed current cathodic protection (ICCP) is an effective and direct method for controlling the corrosion of reinforced concrete (RC) structures. However, few investigations related to ICCP in cracked RC structures have been reported. In this study, the effect of cracks in concrete cover on ICCP of chloride-contaminated RC structures was investigated through a numerical model including steel polarisation, electrode reactions, and ionic migration. In the developed numerical model, cracked concrete cover is assumed to consist of sound concrete and cracks, and cracks have their own ionic diffusion coefficients. The results indicate that the ICCP can maintain its ability to remove Cl^- if concrete cover does not completely crack. Once the complete cracking in concrete cover occurs, the Cl^- removal ability of ICCP would decrease or even disappear. Cracking does not cause any adverse effect on the pH improvement of ICCP. In this case, a stronger cathodic polarisation is recommended.

1. Introduction

The corrosion of reinforcing steel induced by chloride attack or carbonation is a primary cause of the degradation in the durability of reinforced concrete (RC) structures [1–3]. Thus, some techniques have been developed to repair these corrosion-damaged RC structures, such as patch repair, coatings and surface treatments, use of corrosion inhibitor, cathodic protection (CP), electrochemical chloride removal (ECR), electrochemical realkalization (ERA), etc. [4]. Among them, CP, including impressed current cathodic protection (ICCP) and sacrificial anode cathodic protection (SACP), has been demonstrated to be an effective and direct electrochemical method for preventing the corrosion of RC structures [5]. In this method, an electric field is applied to the RC structure, and the reinforcing steel works as a cathode and is polarized [6]. An inert anode and an external power to provide the protection current are required in ICCP [7], while a metal anode that is more active than iron is used in SACP, and the protection current originates from the difference in electrochemical potentials between anode and iron [8]. In general, ICCP is suitable for large RC structures with severe corrosion and long life expectancy while SACP is suitable for RC structures with targeted repairs and short life expectancy [9].

In a practical engineering, cracking of RC structures is inevitable due to external loading, internal shrinkage, freezing-thawing cycles or alkali-aggregate reactions [10]. From the macro level, cracking of concrete lowers its resistivity, which affects the protection current that reinforcing steel receives. Dugarte et al. [11] studied impressed current cathodic prevention for cracked RC structures with different crack widths (ranging from 0.01 to 0.04 in) by measuring the instant-off potentials. They found that cracks had a significant influence on the cathodic polarisation of reinforcing steel in concrete. Note that this is the only investigation concerning the CP for cracked RC structures that has currently been reported, and thus, more related investigations are required.

Cathodic protection (CP) originated in pipelines, steel structures in offshore platforms, and ship hull. Later, it was developed to RC structures. The numerical model of CP based on Laplace equation for the former have also been widely used to investigate RC structures [7,12,13]. In this numerical model, the spatial distribution of electric potential (φ)

* Corresponding author.
** Corresponding author.
E-mail addresses: guobingbing212@163.com (B. Guo), qgf_forever@hit.edu.cn (G. Qiao), Z.li-2@tudelft.nl (Z. Li), lidongsheng@dlut.edu.cn (D. Li), enya_dai@126.com (J. Dai), wangyanwjx@xauat.edu.cn (Y. Wang).

https://doi.org/10.1016/j.jobe.2021.102943
Received 23 April 2021; Received in revised form 30 June 2021; Accepted 1 July 2021
Available online 2 July 2021

Table 1
Parameter values in electrode kinetics reactions at the steel surface.

Parameter	E_{Fe}	E_{O2}	E_{H2}	i_{0_Fe}	i_{0_O2}	i_{0_H2}	b_{Fe}	b_{O2}	b_{H2}
Value	−0.76 V	0.189 V	−1.03 V	7.1×10^{-5} A/m^2	7.7×10^{-5} A/m^2	1.1×10^{-2} A/m^2	4.1 V/a	1.8 V/a	1.5 V/a

All the values are from Muehlenkamp et al. [28].

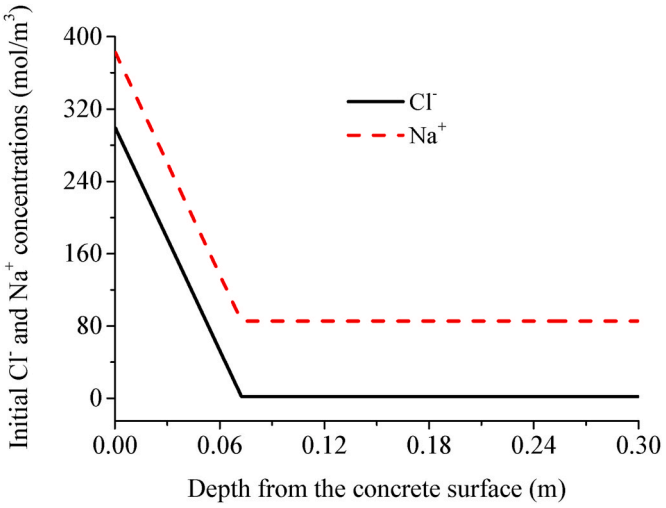

Fig. 1. Initial Cl^- and Na^+ concentrations in concrete pore solution.

in RC structures is related to the resistivity of concrete (ρ) as shown in Eq. (1).

$$\nabla \cdot \frac{1}{\rho} \nabla \varphi = 0 \tag{1}$$

Simultaneously, the nonlinear boundary caused by the steel polarisation is considered to solve the numerical model.

By testing the Cl^- and OH^- concentrations in the concrete pore solution, Hassanein et al. [14] found that CP could cause a significant decrease in the Cl^-/OH^- ratio around the protected steel bar. The study of Polder et al. [15] also indicated that CP could increase the pH. The decrease in the Cl^-/OH^- ratio help the corroded reinforcing steel to return to be passive. The field experimental investigations by Christodoulou et al. [16] indicated that the reinforcing steel could remain passive over two years after the ICCP operation for 5 years. Hence, in addition to the steel polarisation, ICCP has other beneficial effects, such as removing Cl^- and improving the pH at the steel surface in RC structures. However, these great beneficial effects have not been considered in the above numerical model based on Laplace equation. Therefore, to more accurately simulate CP, it is very necessary to develop a numerical model that includes the ionic migration in concrete and the electrode kinetics reactions at the steel surface.

From the micro level, cracks provide additional transport paths for free ions in the concrete, affecting the ionic migration under external electric field. Hence, cracking of concrete cover must affect the Cl^- removal and pH improvement of ICCP. However, no study can be found considering these effects on ICCP for cracked RC structures. In this paper, therefore, a numerical model considering the steel polarisation, electrode reactions and ionic migration is developed to investigate the Cl^- removal and pH improvement of ICCP for cracked RC structures. In the developed numerical model, cracked concrete cover is assumed to consist of sound concrete and cracks, and cracks have their own ionic diffusion coefficients. The remainder of this paper is organised as follows. Section 2 introduces the numerical theory of ICCP related to ionic migration and electrochemical reactions. Section 3 presents a numerical benchmark example of ICCP for sound RC structures. Based on the results in Section 3, a well-designed ICCP system is considered as an example to discuss the effect of cracks in a concrete cover on ICCP in Section 4. Conclusions are presented in Section 5.

2. Numerical theory

When a normal ICCP is applied to RC structures, the potential of the reinforcing steel will have a negative shift, and reduction reaction of oxygen will occur at the steel surface, producing OH^-. Additionally, the free ions in the pore solution of concrete, i.e., Na^+, K^+, Cl^-, OH^-, Ca^{2+}, SO_4^{2-}, etc., are forced to move due to the action of the external electric field. Hence, the numerical model in this study focuses on both of the ionic transport in concrete and the electrochemical reactions at the steel–concrete interface. Ca^{2+} and SO_4^{2-} were not considered because their concentrations in the concrete pore solution were very low [17,18].

2.1. Transport model in cracked concrete

When ICCP is applied to a saturated RC structure, the ionic transport in concrete will be governed by electromigration and diffusion, which can be described using the Nernst-Planck and continuity equations [19,20]:

$$\frac{\partial c_i}{\partial t} = -\nabla \cdot N_i \tag{2}$$

$$N_i = D_i \left(-\nabla c_i - \frac{z_i c_i F}{RT} \nabla \varphi \right) \tag{3}$$

where c_i, N_i, D_i, and z_i are the concentration (mol/m^3), flux (mol/(m^2·s)), diffusion coefficient (m^2/s), and electric charge number (dimensionless) of the free ion i in the concrete pore solution, respectively; φ is the electric potential (V); F is the Faraday constant (9.6485×10^4 C/mol); R is the gas constant (8.314 J/(mol·K)); T is absolute temperature (K). The chloride diffusion coefficient (D_{Cl}) can be easily measured through electrically accelerated test methods [21]. The diffusion coefficients of other ions, such as Na^+, K^+, and OH^-, can be obtained via the following equation:

$$D_i = \frac{D_{Cl}}{D_{Cl\_free}} \cdot D_{i\_free} \tag{4}$$

where D_{i_free} is the diffusion coefficient of the ion i in free water, and their values can be seen in Ref. [22].

In this study, cracked concrete is assumed to consist of sound concrete and cracks. Cracks have their own ionic diffusion coefficients. Several studies [23–25] have indicated that the ionic diffusion coefficient in a crack is closely related to its width. Sahmaran et al. [25] investigated the effect of crack width (from 29.4 μm to 392.0 μm) on the chloride diffusion coefficient, and obtained the following relationship between D_{Cl_cr} (m^2/s) and w_{cr} (μm):

$$D_{Cl\_cr1} = \left(34.58 + 0.002 w_{cr}^2\right) \times 10^{-11} \tag{5}$$

Djerbi et al. [23] obtained the chloride diffusion coefficients of cracks in concrete with the width ranging from 48.18 μm to 241.20 μm. Based on their experimental data, the following relationship was fitted by Du et al. [24]:

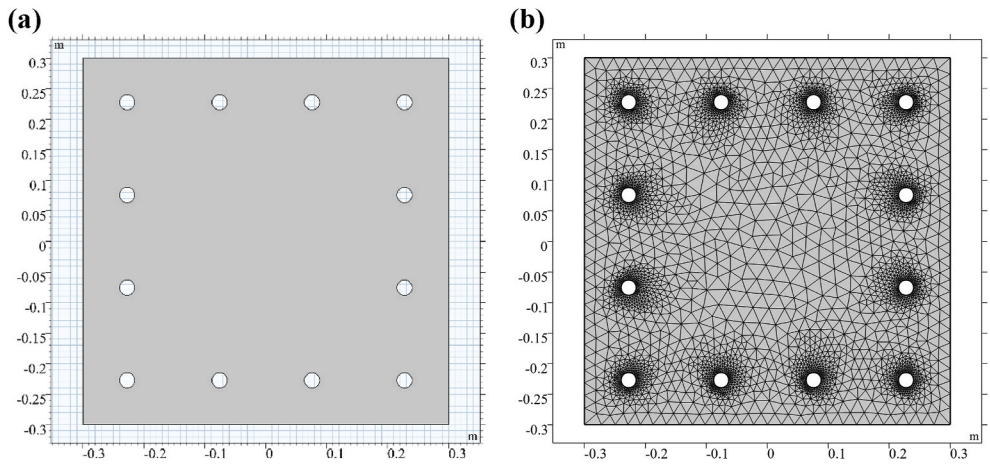

Fig. 2. (a) Geometric model; (b) finite element mesh.

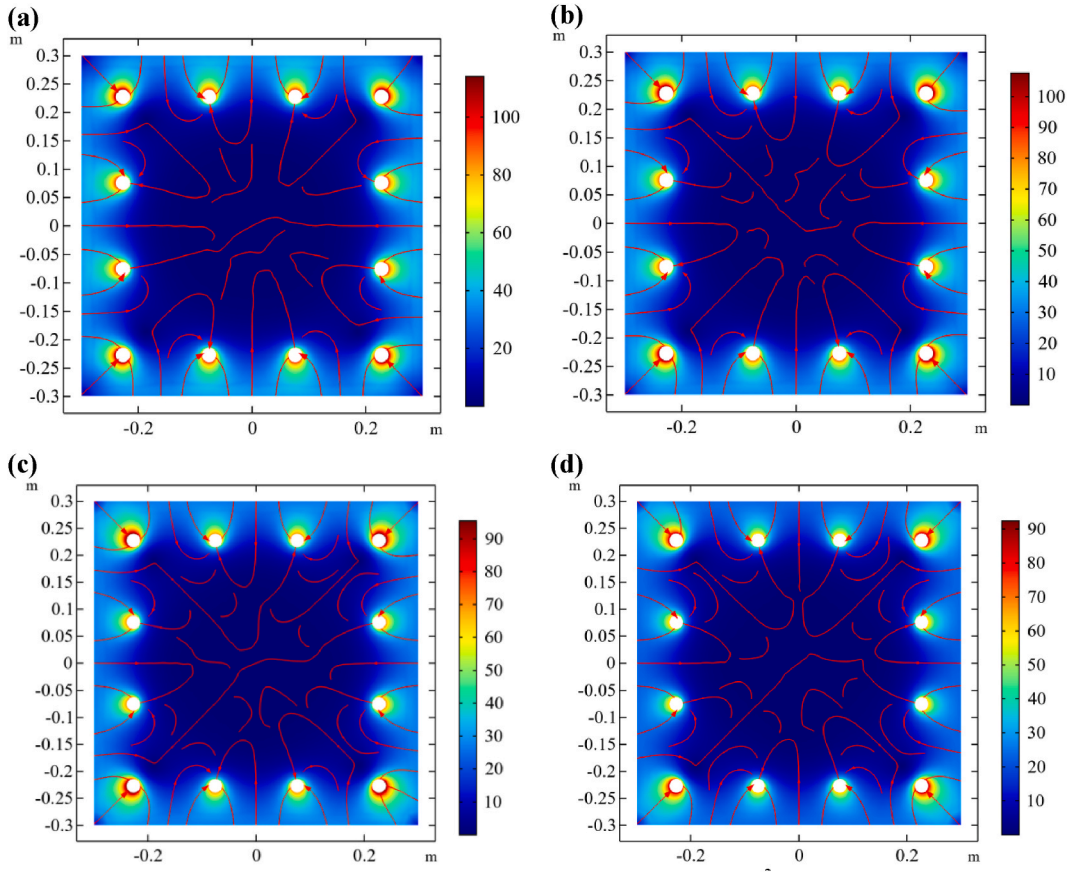

Fig. 3. Current density in RC structure with 0.9-V ICCP (unit: mA/m^2): (a), (b), (c), and (d) show the numerical results at 30 d, 60 d, 90 d and 120 d, respectively.

$$D_{\mathrm{Cl\_cr2}} = \left[128.1 - \frac{72.6}{1 + \left(w_{\mathrm{cr}}/75.8\right)^{4.8}}\right] \times 10^{-11} \tag{6}$$

In the study of Sahmaran et al. [25], cracks were induced by 4-point bending and the cracks were V-shaped. The averaged crack width was adopted. In the study of Djerbi et al. [23], cracks were induced by controlled splitting test and the tortuosity of cracks was neglected. Their methods to obtain the chloride diffusion coefficient in crack were of limited accuracy. Thus, there is a large discrepancy between the chloride diffusion coefficients calculated from these two equations. For instance, when the crack width is 300 μm, $D_{\mathrm{Cl\_cr1}}$ calculated via Eq. (5) is 2.15 × 10^{-9} m^2/s, which is even more than that in free water (2.03 × 10^{-9} m^2/s), and $D_{\mathrm{Cl\_cr2}}$ in Eq. (6) is 1.28 × 10^{-9} m^2/s. To reduce the uncertainty regarding the chloride diffusion coefficient of a crack, the average value of Eqs. (6) and (7) was used in this study [24]:

$$D_{\mathrm{Cl\_cr}} = \frac{D_{\mathrm{Cl\_cr1}} + D_{\mathrm{Cl\_cr2}}}{2} \tag{7}$$

Theoretically, $D_{\mathrm{Cl\_cr}}$ should have lower and upper limits, which are closely related to crack width. According to experimental results in Ref. [25], when crack width is less than 50 μm, cracking of concrete hardly affects the diffusion coefficient of chloride in concrete. Hence, in this situation, $D_{\mathrm{Cl\_cr}}$ was assumed to be equal to the diffusion coefficient of chloride in sound concrete, and the effect of crack on the chloride diffu-

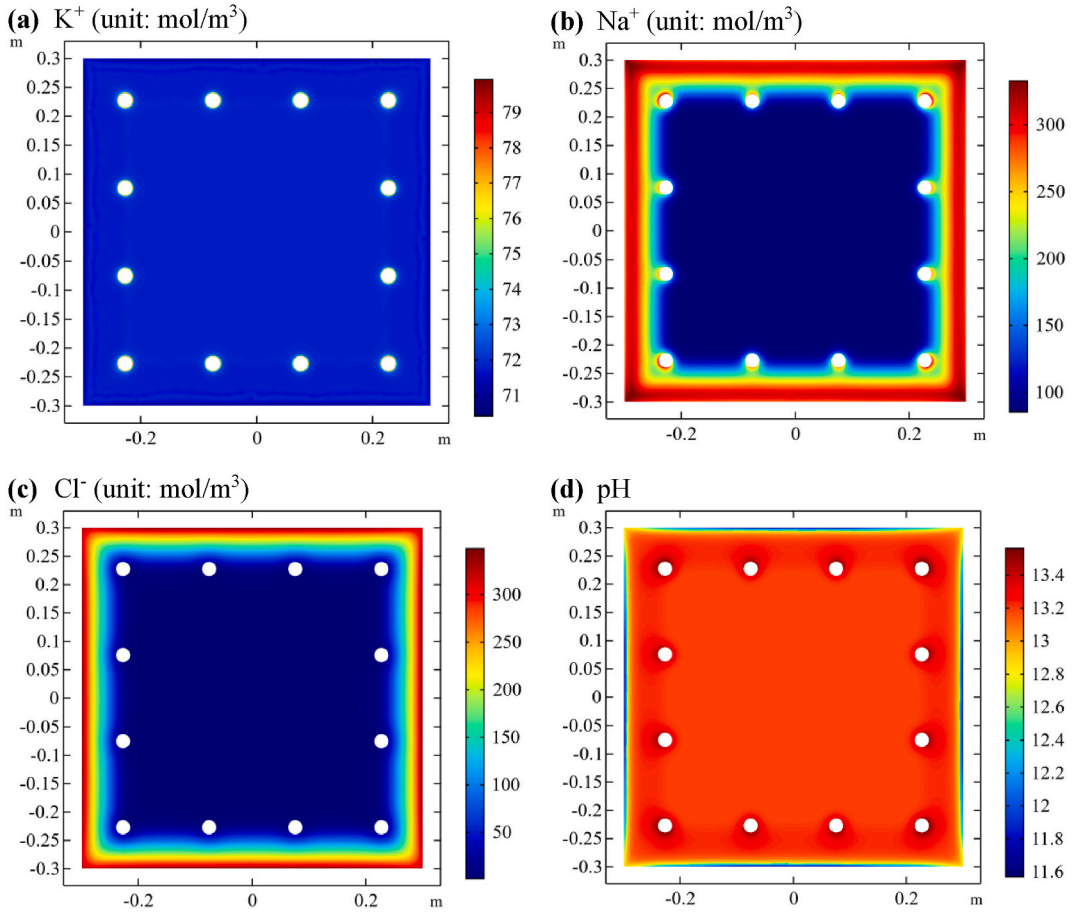

Fig. 4. Ionic concentrations and pH in RC structure when the 0.9-V ICCP runs for 90 d: (a) the K^+ concentration; (b) Na^+ concentration; (c) the Cl^- concentration; (d) the pH.

sivity was neglected in this study. When the diffusion coefficient of chloride in cracks calculated via Eq. (7) was more than that in free water (2.03×10^{-9} m^2/s), the effect of crack wall on the chloride diffusion in pore solution was assumed be neglected, and D_{Cl_cr} was defined to be 2.03×10^{-9} m^2/s.

The quantitative relationship between chloride diffusion coefficient and crack width used in the study is a kind of rough approximation. The assumption about the limits of D_{Cl_cr} may be unreasonable. When the crack width is 348 μm, the average value of Eqs. (5) and (6) will be 2.03×10^{-9} m^2/s, which is equal to the chloride diffusion coefficient in free water. However, according to the relationship (i.e., Eq. (5)) obtained by Sahmaran et al. [25], D_{Cl_cr} is 2.77×10^{-9} m^2/s with the crack width of 348 μm, which is far more than the chloride diffusion coefficient in free water. In addition, according to the obtained relationship (i.e., Eq. (6)) based on crack width ranging from 48.18 μm to 241.20 μm [23,24], the maximum D_{Cl_cr} is 1.281×10^{-9} m^2/s, which is far less than the chloride diffusion coefficient in free water, and this relationship does not suitable for crack with a larger width. Therefore, it is necessary to carry out a series of experimental research to obtain the whole and accurate relationship between the chloride diffusion coefficient in concrete crack and its width in the further work.

The directed movement of free ions in the concrete pore solution produces an electric current. Thus,

$$I = F\sum_{i=1}^{n} z_i N_i = F\sum_{i=1}^{n} z_i D_i \left(-\nabla c_i - \frac{z_i c_i F}{RT}\nabla\psi\right) \tag{8}$$

where I is the current density (A/m^2). Based on the continuity equation, the current density should satisfy the following equation:

$$\nabla \cdot I = 0 \tag{9}$$

When chloride enters concrete from the external environment, it can be physically and chemically bound by cement hydrates. The chloride binding behaviour significantly affects the ionic transport in concrete, which can be described by four types of chloride binding isotherms, i.e., linear, Langmuir, Freundlich, and BET binding isotherm [26]. The Langmuir isotherm which is commonly applied in numerical models due to the easiness to get analytical solution was used in this study [27].

$$s_{Cl} = \frac{\alpha c_{Cl}}{1 + \beta c_{Cl}} \tag{10}$$

where s_{Cl} is the concentration of bound chloride; α and β are constants that can be obtained from experiments.

2.2. Electrode kinetics reactions

When ICCP is applied to RC structures, electrode kinetics reactions will occur at the steel-concrete interface to transform ionic conduction in concrete into electronic conduction in reinforcing steel [28]. Generally, the reduction of oxygen should be dominant:

$$O_2 + 2H_2O + 4e^- \rightarrow 4OH^- \tag{11}$$

But if the applied external electric field of ICCP is too small, the reinforcing steel will be not completely protected so that oxidation of iron may occur, and even dominate:

$$Fe - 2e^- \rightarrow Fe^{2+} \tag{12}$$

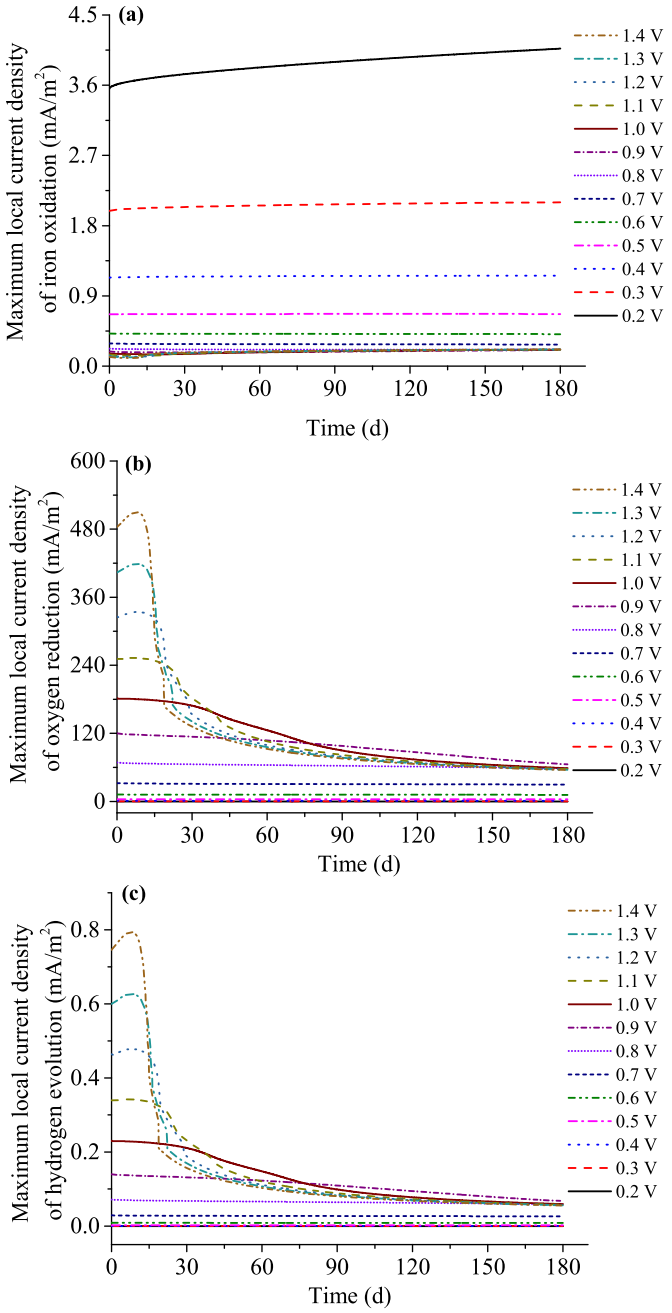

Fig. 5. Maximum local current densities at steel surface in the sound RC structure under different ICCP electric fields: (a) the iron oxidation; (b) the oxygen reduction; (c) the hydrogen evolution.

If the applied electric field is very large, it will be possible that hydrogen evolution occurs:

$$Fe - 2e^{-} \rightarrow Fe^{2+} \tag{13}$$

The reduction of oxygen and the evolution of hydrogen contribute to improvement in the pH around the reinforcing steel. However, the evolution of hydrogen can cause hydrogen embrittlement in steel. Thus, the oxidation of iron and the evolution of hydrogen should be avoided when designing ICCP.

In this study, the Tafel equation was used to calculate the local current densities at the steel–concrete interface caused by the electrode reactions [28]:

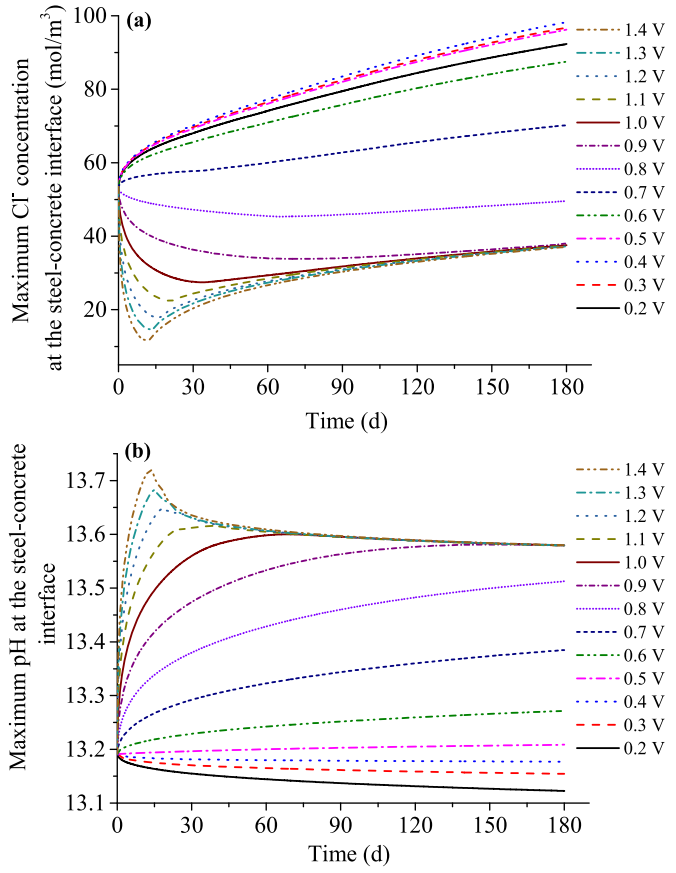

Fig. 6. Maximum Cl^- concentration and pH at the steel surface in the sound RC structure under different ICCP electric fields: (a) the Cl^- concentration; (b) the pH.

$$i_{O_2} = i_{0\_O_2} \exp\left(\frac{-2.3\left(E_c - E_{eq\_O_2}\right)}{b_{O_2}}\right) \tag{14}$$

$$i_{Fe} = i_{0\_Fe} \exp\left(\frac{2.3\left(E_c - E_{eq\_Fe}\right)}{b_{Fe}}\right) \text{ and} \tag{15}$$

$$i_{H_2} = i_{0\_H_2} \exp\left(\frac{-2.3\left(E_c - E_{eq\_H_2}\right)}{b_{H_2}}\right) \tag{16}$$

Here, i_{O2}, i_{0_O2}, E_{eq_O2} and b_{O2} represent the current density, exchange current density, equilibrium potential, and Tafel slope, respectively, in the oxygen reduction reaction; i_{Fe}, i_{0_Fe}, E_{eq_Fe} and b_{Fe} represent the current density, exchange current density, equilibrium potential, and Tafel slope, respectively, in the iron oxidation reaction; i_{H2}, i_{0_H2}, E_{eq_H2} and b_{H2} are the current density, exchange current density, equilibrium potential, and Tafel slope, respectively, in the hydrogen evolution reaction. The parameter values are listed in Table 1.

The oxygen concentration at the steel–concrete interface plays a vital role in the electrode reactions, especially for underwater RC structures. In this study, we primarily focus on the effect of cracks on ICCP, and the oxygen is assumed to be sufficient.

In addition, the sum of the above mentioned three local currents should be equal to the current from the concrete at the steel–concrete interface:

$$\int_s i = \int_s i_{Fe} + \int_s i_{O_2} + \int_s i_{H_2} \tag{17}$$

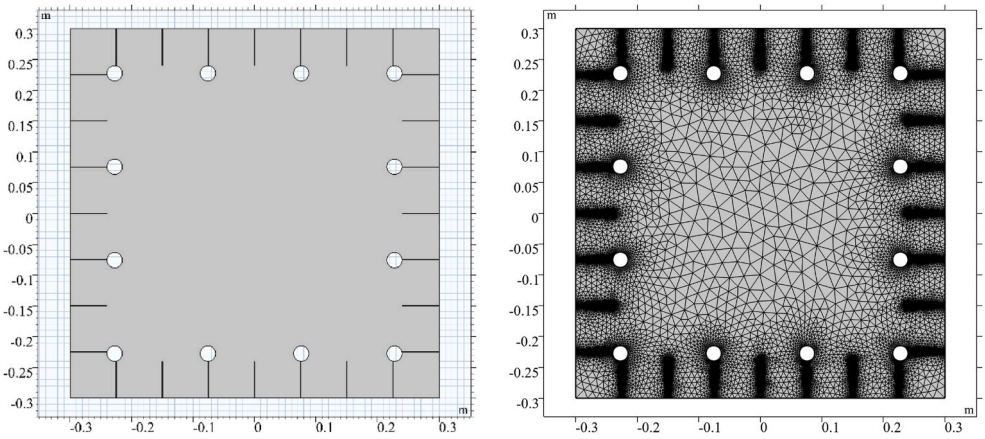

Fig. 7. (a) Geometric model of cracked RC structures; (b) the corresponding finite element mesh.

where *s* denotes the surface area of reinforcing steel.

At the anode–concrete interface, the evolution reactions of oxygen ($4OH^- - 4e^- \rightarrow 2H_2O + O_2$) and chlorine ($2Cl^- - 2e^- \rightarrow Cl_2$) may occur. Generally, the evolution reaction of oxygen is dominant. The nonlinear polarisation at the anode-concrete interface can be neglected [28]. The anodic reactions can decrease the pH of concrete pore solution around the anode, which may produce an acidification damage [29]. This may affect the chloride binding behaviors, which is not considered.

3. ICCP for sound RC structures

3.1. Computational model

A chloride-contaminated RC pillar was used as a benchmark example in this study. The cross-section was square with dimensions of 600 × 600 mm^2. The diameter of the longitudinal steel bar was 25 mm, and 12 steel bars were embedded in the concrete. The thickness of concrete cover for the longitudinal bars was 60 mm. The RC pillar was exposed to a 300–mol/m^3 chloride environment. The depth of chloride penetration was 72.5 mm, indicating that Cl^- had already penetrated to the steel surface. The Cl^- concentration in concrete pore solution had a linear relationship with the penetration depth, as shown in Fig. 1. The ICCP was adopted to prevent the corrosion of this RC pillar. Actually, the steel bars in the RC pillar consist of longitudinal bars and stirrups. Stirrups are easier to be corroded than longitudinal bars. But when applying ICCP, stirrups are closer to anode and can receive more protection current [12], and thus stirrups are easier to be protected. In addition, considering that pillar is a compressive member, longitudinal bars in a RC pillar are stressed while the arrangement of stirrups only meets the constructional requirement. From the perspective of structural safety, longitudinal bars are more important. Therefore, to shorten the calculation time of the numerical model, the cross section without the stirrups in RC pillar were chosen.

The numerical model based on the above theoretical equations was used to design ICCP for this chloride-contaminated RC pillar. A cement-based conductive anode was used in the ICCP. The K^+ concentration and pH value in the concrete pore solution were 71.79 mol/m^3 and 13.19, respectively. The Cl^- and Na^+ concentrations in the central area of this pillar where the external chloride could not penetrate were 2.04 mol/m^3 and 83.51 mol/m^3, respectively. The chloride diffusion coefficient was 8.9 × 10^{-12} m^2/s. The values of α and β in Eq. (10) were 0.98 and 0.29, respectively. These values were determined by referring to Elakneswaran et al. [30], Zibara [31] and Guo [32].

The effect of the variation in environmental conditions on a current-controlled ICCP (such as temperature and humidity) is smaller than a voltage-controlled ICCP, and thus, the current-controlled ICCP is more common in practical engineering. The variation in the resistivity of concrete cover directly affects the output current of power supply in a voltage-controlled ICCP while it affects the output voltage in a current-controlled ICCP. Cracking of concrete affects its resistivity, and it can be inferred that the effect of cracks in a voltage-controlled ICCP is more significant and complicated than a current-controlled ICCP. Therefore, a two-dimensional numerical model of the voltage-controlled ICCP was built, as illustrated in Fig. 2(a). A free triangle was used to mesh the geometrical model. The mesh at the steel surface was more refined, as shown in Fig. 2(b). Considering that the cement-based conductive anode was directly paved at the outer surface of the RC pillar, the outer surface was defined as the anode–concrete boundary. At the steel–concrete interface, the electrode reactions, including iron oxidation, oxygen reduction, and hydrogen evolution were considered. The voltage was applied between the anode and the reinforcing steel. Thus, all the boundaries in Fig. 2(a) were assumed to be insulated. COMSOL Multiphysics was used to solve the numerical model. The numerical results, including the temporal and spatial distributions of the ionic concentration, current density and electric potential in concrete, and the local current densities at the steel surface, can be obtained. The numerical results related to the steel–concrete interface will be discussed in detail because they directly reflect the corrosion control effect while some other numerical results will be simply introduced.

3.2. Results and discussion

The corrosion control effects of ICCP, i.e., the cathodic polarisation, the Cl^- concentration and pH value in the vicinity of the reinforcing steel, are determined by the current density that ICCP delivers to RC structures. From the macro level, the current density depends on the output voltage and the concrete resistivity, and the resistivity is material attribute. Thus, the corrosion control effects of ICCP in given RC structures are determined by the size of the output voltage, which will be predicted via the numerical model.

The distributions of the current density in RC structures for the 0.9-V ICCP at different times is shown in Fig. 3. The reason for selecting the 0.9-V voltage will be presented later. It can be seen that the current flows to reinforcing steel from anode. The current density delivered by ICCP to reinforcing steel decreases as the ICCP runs. Generally, the outside surface of the reinforcing steel toward the concrete cover surfers from more serious corrosion than the opposite surface because it is closer to the external environment. Thus, the outside surface requires to receive more protection current [12]. This is also observed in Fig. 3. Fig. 4 presents the distributions of the ionic concentrations at different times. It can be observed that the ICCP application causes the migration of cations toward the reinforcing steel and the acidification at the anode-concrete interface. These adverse effects have been confirmed by some published experimental results [33,34]. In addition, it is found in

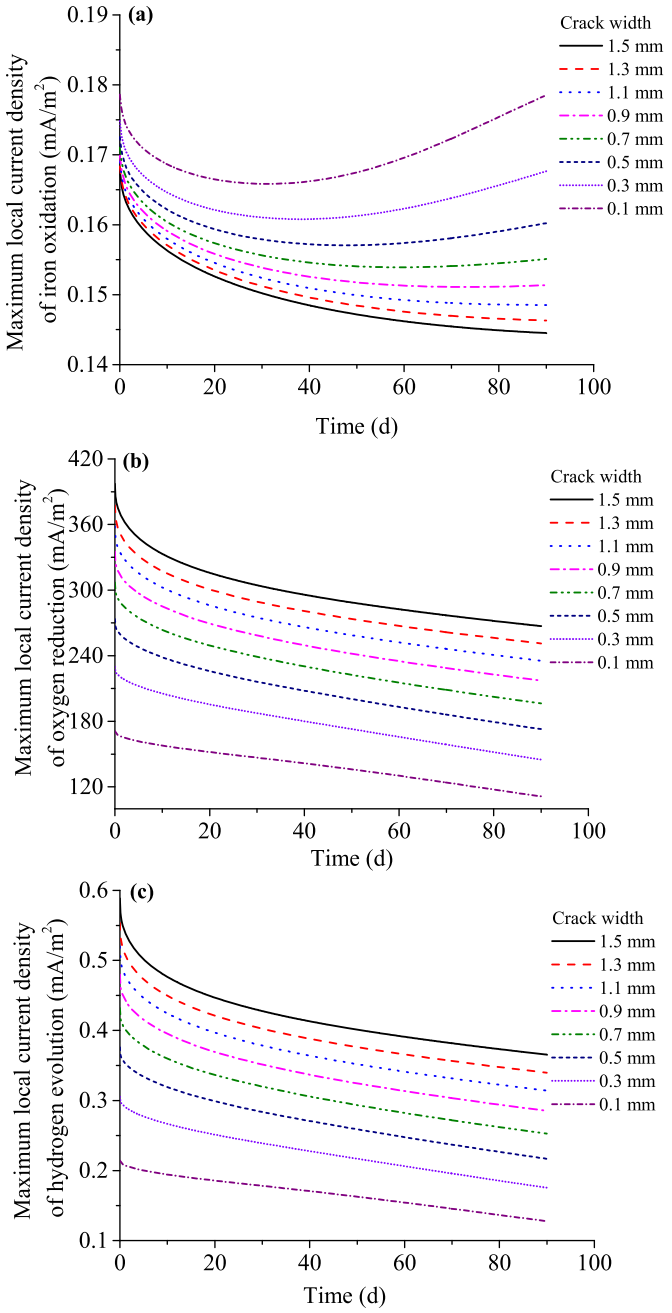

Fig. 8. Maximum local current densities at steel surface with different crack widths: (a) the iron oxidation; (b) the oxygen reduction; (c) the hydrogen evolution.

Figs. 3 and 4 that the maximum values of current density, Cl^- concentration and pH representing the corrosion control effect, are located on the outside surface. We primarily discuss these maximum values.

Fig. 5 illustrates the maximum local current densities of each type of electrode reactions under different externally applied electric fields. When the external electric field is relatively small, the local current density of iron oxidation is larger (Fig. 5(a)), indicating that it is possible that the reinforcing steel cannot be completely protected. Generally, when the corrosion current density is greater than 2 mA/m^2, the reinforcing steel is assumed to be active [35]. Thus, it can be inferred from the numerical results in Fig. 5(a) that an applied electric field that is greater than 0.3 V can overcome the potential difference between the anode and the steel, and the steel corrosion is then arrested. Moreover, with an increase in the applied electric field, oxygen reduction is dominant, and iron oxidation is completely suppressed. Simultaneously, hydrogen evolution gradually emerges. When the applied electric field is greater than 1.0 V, hydrogen evolution becomes more obvious, which may cause hydrogen embrittlement of the reinforcing steel, especially in the early stage of the ICCP operation. Thus, according to the local current densities, the applied electric field in ICCP for the chloride-contaminated pillar is recommended to be between 0.3 V and 1.0 V.

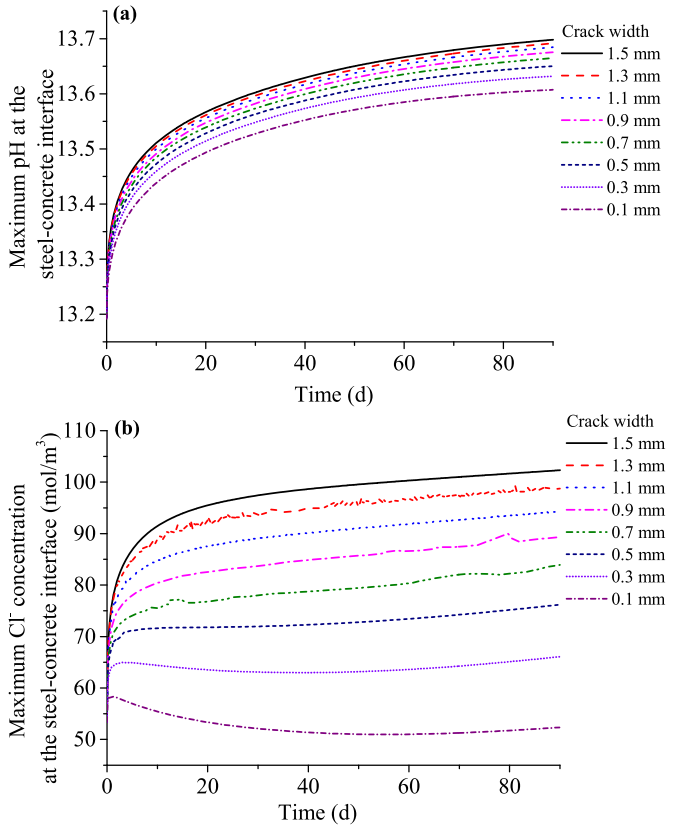

Fig. 9. Maximum pH and Cl^- concentration at the steel surface with different crack widths: (a) the pH; (b) the Cl^- concentration.

The local current densities, particularly those produced by oxygen reduction and hydrogen evolution, vary significantly when ICCP begins to operate. However, when the operation time is over 90 d, the local current densities tend to be stable. The application of ICCP can cause the ionic migration and the electrode reactions. Directed ionic migration produces the current, which is also the protection current that ICCP delivers into RC structures. The current density at the steel–concrete interface determines the electrode reaction. The electrode reactions can produce or consume part of free ions, such as OH^-, in turn affecting the ionic transport. Therefore, a balance between the ionic transport and the electrode reactions is reached after 90 d of the ICCP operation.

Fig. 6 shows the maximum Cl^- concentration and pH in the vicinity of the reinforcing steel. It is observed that the control effect of ICCP on these kinetic factors is increasingly significant with an increase in the applied voltage. The effect of the concentration gradient on the Cl^- transport in concrete is greater than that of the potential gradient when the external electric field is smaller. Thus, when the applied voltage in this benchmark example is less than 0.7 V, some chloride ions can still penetrate to the steel surface, but the penetration rate significantly decreases. The OH^- concentration gradient is small when ICCP begins to run, and OH^- moves toward the anode. The amount of OH^- produced at the steel–concrete interface is less than the amount of OH^- migrated when a smaller external electric field is applied. Hence, it can be seen that when the applied voltage is less than 0.4 V, the pH value in the vicinity of the steel bar decreases slightly (Fig. 6), operating against the

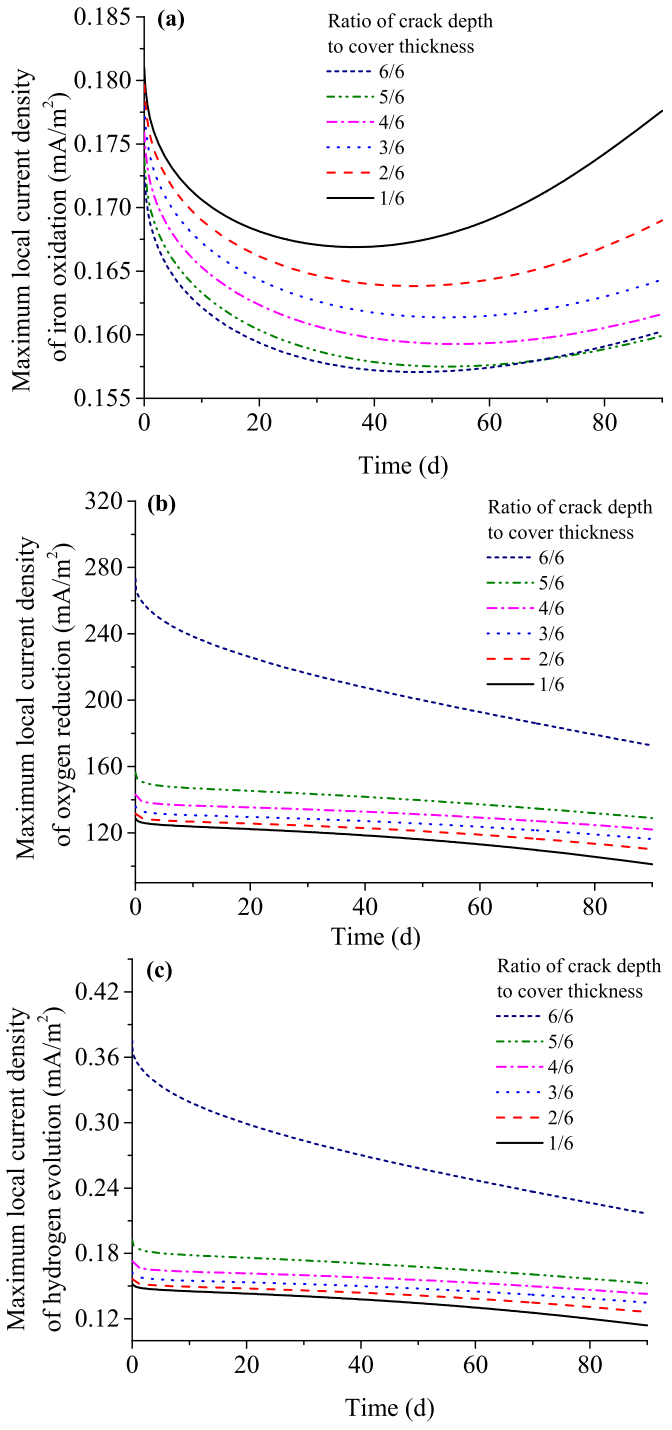

Fig. 10. Maximum local current density at steel surface with different crack depths: (a) the iron oxidation; (b) the oxygen reduction; (c) the hydrogen evolution.

ICCP. However, this adverse effect can be ignored. Although ICCP with a smaller electric field can provide sufficient cathodic polarisation, it cannot prevent Cl^- penetration and improve the pH at the steel surface. Thus, there is still a risk that the corrosion of reinforcing steel is re-aroused. For chloride-contaminated RC structures, the applied electric field of the ICCP should be enough large to ensure that it can lower the Cl^- concentration in the vicinity of the reinforcing steel. In this benchmark example, when the applied voltage is greater than 0.6 V, ICCP can significantly improve the pH value in the vicinity of the reinforcing steel. When the applied voltage is greater than 0.8 V, ICCP can signifi-

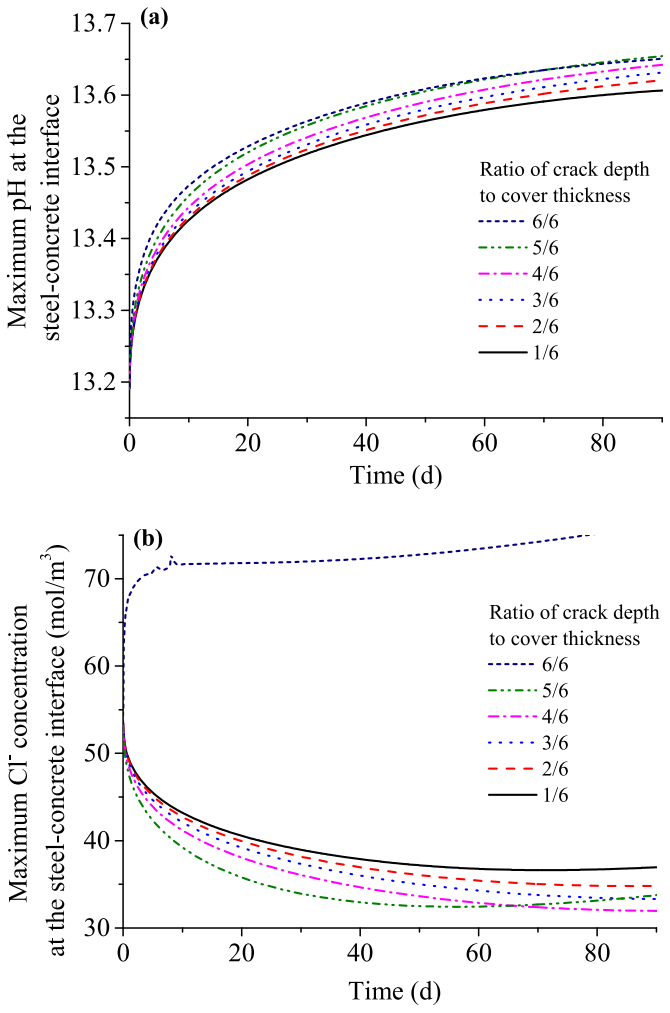

Fig. 11. Maximum pH and Cl^- concentration at steel surface with different crack depths: (a) the pH; (b) the Cl^- concentration.

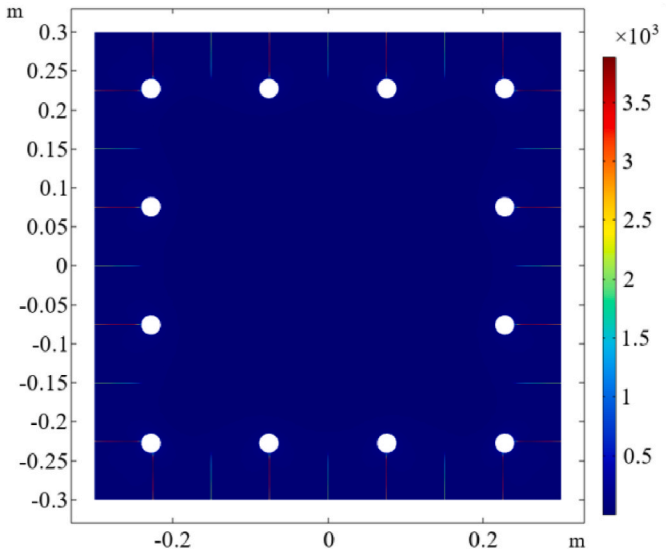

Fig. 12. Current density in cracked RC structure when the 0.9-V ICCP runs for 90 d (unit: mol/m³) (the width and depth of crack are 0.5 mm and 60 mm).

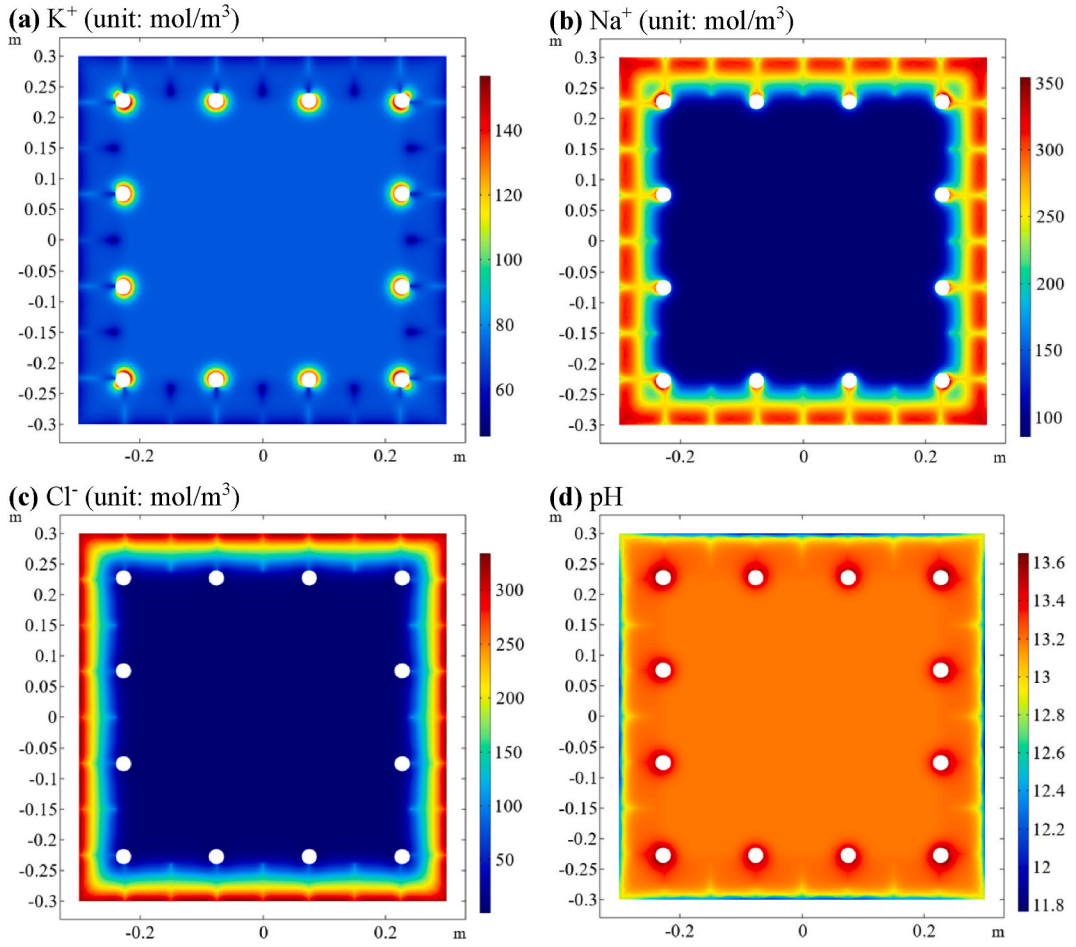

Fig. 13. Ionic concentrations in cracked RC structure when the 0.9-V ICCP runs for 90d (the width and depth of crack are 0.5 mm and 60 mm, respectively): (a) the K^+ concentration; (b) Na^+ concentration; (c) the Cl^- concentration; (d) the pH.

cantly reduce the Cl^- concentration. Therefore, a 0.9-V electric field is suggested in this benchmark example.

Fig. 6 shows that ICCP with an electric field greater than 1.0 V has a strong ability to lower the Cl^- concentration in the vicinity of the steel bar and to improve the pH. After a period of the ICCP operation, the Cl^- concentration and pH values are nearly constant. Continuing to run ICCP at this moment does not further decrease the Cl^- concentration or increase the pH. Thus, we conclude that increasing the applied electric field or prolonging the running time does not work on controlling the kinetics factors when ICCP operates over a long period of time. Conversely, long-term ICCP operation may cause some adverse effects, such as a decrease in the steel–concrete interfacial bond strength [34], and acidification damage in the vicinity of the anode [33]. The experimental results of Christodoulou et al. [16] also indicated that the reinforcing steel can remain in a passive state for a long time after interrupting the ICCP. Therefore, it is suggested to interrupt ICCP when it runs for a long time, and ICCP can rerun when the reinforcing steel is re-active, which is similar to an intermittent CP [14,36]. The numerical model including the ionic transport and electrochemical reactions can be used to design and investigate the intermittent CP for RC structures.

4. ICCP for cracked RC structures

4.1. Computational model

Introducing artificial cracks has been proven a simple and controllable method to investigate the effect of cracks on the durability of RC structures [37]. Thus, seven artificial cracks were introduced evenly on each side in this study, as illustrated in the geometric model (Fig. 7(a)). The initial parameters, boundary conditions, and finite element mesh are the same as in Section 3.1. The mesh in crack domain is refined, as shown in Fig. 7(b).

The width and depth of crack are two key parameters affecting ionic transport in concrete. The results in Section 3 indicate that ICCP with a 0.9-V electric field applied for 90 d can achieve a good corrosion control. Therefore, we mainly discuss the effect of these parameters on this well-designed ICCP.

4.2. Effect of crack width on ICCP of RC structures

In this section, we discuss the effect of crack width on the ICCP of cracked RC structures. It is assumed that the concrete cover completely cracks, which means that the depths of cracks are equal to the thickness of the concrete cover. The numerical model predicts the local current densities at the steel–concrete interface under different crack widths; the maximum values are shown in Fig. 8. With an increase in the crack width, the local current density of iron oxidation exhibits a decreasing trend (Fig. 8(a)); the local current densities of oxygen reduction and hydrogen evolution exhibit an increasing trend (Fig. 8(b) and (c)). The width of the crack directly affects the protection current that the reinforcing steel receives. When the crack width in concrete cover is larger, the reinforcing steel receives more protection current, and then will have a stronger cathodic polarisation. Fig. 9 illustrates the maximum pH and Cl^- concentration at the steel–concrete interface. Cracking of the concrete cover facilitates the reduction reaction of oxygen at the steel surface, improving the pH value at the steel–concrete interface

with increasing the crack width (Fig. 9(a)). The 0.9-V ICCP for the sound RC pillar has a strong ability to lower the Cl^- concentration in the vicinity of the reinforcing steel. However, for cracked RC pillar, this ability significantly decreases until to disappear. When the crack width is greater than 0.3 mm, ICCP cannot lower the Cl^- concentration (Fig. 9 (b)); conversely, the Cl^- concentration increases, gradually, reaching a stable state as the ICCP runs. Thus, a well-designed ICCP may lose its ability to remove Cl^- when concrete cover completely cracks.

4.3. Effect of crack depth on ICCP of RC structures

Artificial cracks with a width of 500 μm were introduced to investigate the effect of crack depth on the ICCP. The maximum local current densities at the steel surface under different crack depths are shown in Fig. 10. It is observed that an increase in crack depth causes a reduction in the local current density of iron oxidation, and a rise in the local current densities of oxygen reduction and hydrogen evolution. In particular, the local current densities of oxygen reduction and hydrogen evolution increase significantly when concrete cover completely cracks. Thus, the crack depth affects the protection current that ICCP delivers to the reinforcing steel, and the reinforcing steel receives stronger cathodic polarisation as the crack depth in the concrete cover increases.

Fig. 11 illustrates the maximum pH and Cl^- concentration at the steel–concrete interface. In Fig. 11(a), the pH value increases as the ICCP operates, regardless of the crack depth. With a greater the crack depth, the increasing trend in the pH value is stronger. When the concrete cover does not completely crack, the gradient of electric potential in concrete cover, especially in cracks, becomes larger, and the driving force of ionic electromigration has an increase. This means that the ability of ICCP to remove Cl^- in the vicinity of the reinforcing steel is improved with increasing crack depth (Fig. 11(a)). However, it is available for external Cl^- to take these thorough pathways when the concrete cover completely cracks, and the Cl^- concentration at the steel–concrete interface increases significantly although the gradient of the electric potential becomes stronger. This point will be further discussed in Section 4.4.

4.4. Current density and ionic concentration in cracked RC structure with ICCP

The current density and ionic concentrations in the cracked RC structure when the 0.9-V ICCP runs for 90 d are presented in Figs. 12 and 13. It is observed in Fig. 12 that the current density in the cracks is much higher than that in other areas; the highest current density is located into the cracks facing the reinforcing steel. In Fig. 13, it is seen that cracks provide additional paths for ionic transport. The maximum Cl^- concentration and pH value in the vicinity of the reinforcing steel were also located into the cracks. In addition, the pH value at the anode–concrete interface is less than 11.8 due to the evolution reaction of oxygen.

4.4. Discussion

Cracking of concrete cover provides more transport pathways for free ions and external aggressive species (such as Cl^-, oxygen, water, carbon dioxide, etc.). Note that the effect of carbonation on the pH has not been taken into account in this study. Since external aggressive species penetrate into concrete cover more easily, it means that reinforcing steel needs to receive a stronger cathodic polarisation to avoid the corrosion initiation or being further corroded. In this view, cracking of the concrete cover is harmful for ICCP of RC structures. However, from the insight of the macro level, cracking of concrete cover decreases the resistivity of concrete. It not only increases the driving force of ionic electromigration, but also helps the reinforcing steel to receive more protection current in a voltage-controlled ICCP system or to lower the output voltage in a current-controlled ICCP, which benefits ICCP. In the experimental investigations by Dugarte et al. [11], a total of 30 cracked RC prisms (in which concrete cover completely cracked) were exposed to a 5% NaCl environment to study the effect of cracks on ICCP. The results indicated that the steel bars needed to be more strongly polarized to prevent the corrosion initiation regardless of the crack width. Combining this with the numerical results in Figs. 9(b) and Fig. 11(b), it can be attributed to that the well-designed ICCP of sound RC structures may not prevent the penetration of external Cl^- when the concrete cover completely cracks, and then, the reinforcing steel needs to receive larger protection current density. However, when concrete cover does not completely crack, cracks have little influence on the ability of the well-designed ICCP to remove Cl^- and improve pH (Fig. 11), and in fact, they benefit the ICCP to some extent.

In this study, the amount of the oxygen at the steel surface is assumed to be sufficient, which may be unreasonable particularly for these RC structures located in underwater region. The oxygen concentration at the steel–concrete interface directly affects the electrode kinetics reactions [28], which determines the nonlinear polarisation boundary. However, this study primarily focuses on the effect of cracks in concrete cover on ICCP, and the oxygen transport may need to be considered in future study. When the oxygen concentration is very low, oxygen reduction will be limited. Herein, the numerical model may overestimate the local current density of oxygen reduction. In addition, when the oxygen concentration affects the electrode kinetics reactions, it increases the Ohmic drop at the steel–concrete interface and then decreases the protection current density that ICCP delivers to RC structures. Thus, the numerical model in this study may overestimate the ability of ICCP to remove Cl^- and to increase the pH.

5. Conclusions

A numerical model including steel polarisation, electrode reactions and ionic migration was developed to investigate the ICCP of sound and cracked RC structures. Based on the designed ICCP for sound RC pillar, the effects of crack width and depth in the concrete cover on the ICCP were discussed. The following conclusions are drawn.

The applied electric field in ICCP should be large enough to reduce the Cl^- concentration in the vicinity of the reinforcing steel for chloride-contaminated RC structures. After a long-term operation of ICCP, elevating the applied electric field or prolonging the running time does not remove Cl^- or improve the pH effectively.

In the well-designed ICCP of RC structures, cracking of the concrete cover does not cause any adverse effect on the cathodic polarisation and the pH improvement. However, this Cl^- removal ability of the ICCP decreases and even disappears once the concrete cover completely cracks and the decreasing trend becomes stronger with increasing crack width. In this case, the reinforcing steel needs to have a stronger cathodic polarisation. When the concrete cover does not completely crack, the ability of the ICCP to remove Cl^- is not reduced, and conversely, it is improved to some extent.

Data availability statement

The COMSOL model and data that support the findings of this study are available from the author G. Qiao upon reasonable request.

Credit author statement

Bingbing Guo: Numerical simulation, Analysis, Writing-Original draft preparation, Funding acquisition. Guofu Qiao: Methodology, Writing-Review and Editing, Project administration, Funding acquisition. Zhenming Li: Conceptualization, Analysis, Methodology, Writing-Review and Editing. Dongsheng Li: Conceptualization, Writing-Review and Editing. Jinghui Dai: Methodology, Writing-Review and Editing.

Yan Wang: Conceptualization, Methodology, Writing-Review and Editing.

Declaration of competing interest

The authors declare that they have no known competing financial interests or personal relationships that could have appeared to influence the work reported in this paper.

Acknowledgements

It is highly appreciated for the funding from the National Key Research and Development Program of China (Project No.: 2018YFC0705606), the Nature Science Foundation of China (Project No.: 51908453 and 51578190), the Scientific Research of Shanxi Provincial Department of Education (Project No.: 20JK0710), the China Postdoctoral Science Foundation (Project No.: 2020T130497 and 2020M673607XB), the Independent Research and Development project of State Key Laboratory of Green Building in Western China (Project No.: LSZZ202113).

References

[1] C.L. Page, K.W.J. Treadaway, Aspects of the electrochemistry of steel in concrete, Nature 297 (297) (1982) 109-1982.
[2] U. Angst, B. Elsener, C.K. Larsen, Ø. Vennesland, Critical chloride content in reinforced concrete—A review, Cement Concr. Res. 39 (12) (2009) 1122–1138, https://doi.org/10.1016/j.cemconres.2009.08.006.
[3] X. Liu, D. Niu, X. Li, Y. Lv, Effects of $Ca(OH)_2$–$CaCO_3$ concentration distribution on the pH and pore structure in natural carbonated cover concrete: a case study, Construct. Build. Mater. 186 (2018) 1276–1285, https://doi.org/10.1016/j.conbuildmat.2018.08.041.
[4] A. Goyal, H.S. Pouya, E. Ganjian, P. Claisse, A review of corrosion and protection of steel in concrete, Arabian J. Sci. Eng. 43 (10) (2018) 5035–5055, https://doi.org/10.1007/s13369-018-3303-2.
[5] A. Byrne, N. Holmes, B. Norton, State-of-the-art review of cathodic protection for reinforced concrete structures, Mag. Concr. Res. 13 (68) (2016) 664–677 https://doi.org/2016.10.1680/jmacr.15.00083.
[6] U.M. Angst, A critical review of the science and engineering of cathodic protection of steel in soil and concrete, CORROSION JOURNAL.ORG. 12 (75) (2019) 1420–1433.
[7] M.M.S. Cheung, C. Cao, Application of cathodic protection for controlling macrocell corrosion in chloride contaminated RC structures, Construct. Build. Mater. 45 (2013) 199–207, https://doi.org/10.1016/j.conbuildmat.2013.04.010.
[8] L. Bertolini, E. Redaelli, Throwing power of cathodic prevention applied by means of sacrificial anodes to partially submerged marine reinforced concrete piles: results of numerical simulations, Corrosion Sci. 51 (9) (2009) 2218–2230, https://doi.org/10.1016/j.corsci.2009.06.012.
[9] K. Wilson, M. Jawed, V. Ngala, The selection and use of cathodic protection systems for the repair of reinforced concrete structures, Construct. Build. Mater. 39 (SI) (2013) 19–25, https://doi.org/10.1016/j.conbuildmat.2012.05.037.
[10] C. Zhou, K. Li, X. Pang, Geometry of crack network and its impact on transport properties of concrete, Cement Concr. Res. 42 (9) (2012) 1261–1272, https://doi.org/10.1016/j.cemconres.2012.05.017.
[11] M. Dugarte, A.A. Sagüés, K. Williams, Cathodic prevention for reinforcing steel in cracked concrete of chloride contaminated structures, NACE International Corrosion, Dallas, Texas, 2015.
[12] A.M. Hassanein, G.K. Glass, N.R. Buenfeld, Protection current distribution in reinforced concrete cathodic protection systems, Cement Concr. Compos. 24 (2002) 159–167, https://doi.org/10.1016/S0958-9465(01)00036-1.
[13] S. Fonna, S. Huzni, A. Zaim, Simulation of cathodic protection on reinforced concrete using BEM, J. Mech. Eng. 2 (4) (2017) 111–122.
[14] A.M. Hassanein, G.K. Glass, N.R. Burenfeld, Effect of intermittent cathodic protection on chloride and hydroxyl concentration profiles in reinforced concrete, Br. Corrosion J. 34 (4) (1999) 254–261.
[15] R.B. Polder, W.H.A. Peelen, B.T.J. Stoop, E.A.C. Neeft, Early stage beneficial effects of cathodic protection in concrete structures, Mater. Corros. 62 (2) (2011) 105–110, https://doi.org/10.1002/maco.201005803.
[16] C. Christodoulou, G. Glass, J. Webb, S. Austin, C. Goodier, Assessing the long term benefits of impressed current cathodic protection, Corrosion Sci. 52 (8) (2010) 2671–2679, https://doi.org/10.1016/j.corsci.2010.04.018.
[17] Q. Liu, L. Li, D. Easterbrook, J. Yang, Multi-phase modelling of ionic transport in concrete when subjected to an externally applied electric field, Eng. Struct. 42 (2012) 201–213, https://doi.org/10.1016/j.engstruct.2012.04.021.
[18] Q. Liu, D. Easterbrook, J. Yang, L. Li, A three-phase, multi-component ionic transport model for simulation of chloride penetration in concrete, Eng. Struct. 86 (2015) 122–133, https://doi.org/10.1016/j.engstruct.2014.12.043.
[19] J. Xia, L. Li, Numerical simulation of ionic transport in cement paste under the action of externally applied electric field, Construct. Build. Mater. 39 (2013) 51–59, https://doi.org/10.1016/j.conbuildmat.2012.05.036.
[20] Y. Wang, L.Y. Li, C.L. Page, A two-dimensional model of electrochemical chloride removal from concrete, Comput. Mater. Sci. 20 (2) (2001) 196–212, https://doi.org/10.1016/S0927-0256(00)00177-4.
[21] P. Spiesz, H.J.H. Brouwers, Influence of the applied voltage on the rapid chloride migration (RCM) test, Cement Concr. Res. 42 (8) (2012) 1072–1082, https://doi.org/10.1016/j.cemconres.2012.04.007.
[22] W.M. Haynes, D.R. Lide, T.J. Bruno, CRC Handbook of Chemistry and Physics, CRC Press, 2014.
[23] A. Djerbi, S. Bonnet, A. Khelidj, V. Baroghel-bouny, Influence of traversing crack on chloride diffusion into concrete, Cement Concr. Res. 38 (6) (2008) 877–883, https://doi.org/10.1016/j.cemconres.2007.10.007.
[24] X. Du, L. Jin, R. Zhang, Y. Li, Effect of cracks on concrete diffusivity: a meso-scale numerical study, Ocean. Eng. 108 (2015) 539–551, https://doi.org/10.1016/j.oceaneng.2015.08.054.
[25] M. Şahmaran, Effect of flexure induced transverse crack and self-healing on chloride diffusivity of reinforced mortar, J. Mater. Sci. 42 (22) (2007) 9131–9136, https://doi.org/10.1007/s10853-007-1932-z.
[26] Q. Yuan, C. Shi, G. De Schutter, K. Audenaert, D. Deng, Chloride binding of cement-based materials subjected to external chloride environment-A review, Construct. Build. Mater. 23 (1) (2009) 1–13, https://doi.org/10.1016/j.conbuildmat.2008.02.004.
[27] L. Mao, Z. Hu, J. Xia, G. Feng, I. Azim, J. Yang, Q. Liu, Multi-phase modelling of electrochemical rehabilitation for ASR and chloride affected concrete composites, Compos. Struct. 207 (2019) 176–189, https://doi.org/10.1016/j.compstruct.2018.09.063.
[28] E.B. Muehlenkamp, M.D. Koretsky, J.C. Westall, Effect of moisture on the spatial uniformity of cathodic protection of steel in reinforced concrete, Corrosion 61 (6) (2005) 519–533.
[29] W. Guo, J. Hu, Y. Ma, H. Huang, S. Yin, J. Wei, Q. Yu, The application of novel lightweight functional aggregates on the mitigation of acidification damage in the external anode mortar during cathodic protection for reinforced concrete, Corrosion Sci. 165 (2020) 108366, https://doi.org/10.1016/j.corsci.2019.108366.
[30] Y. Elakneswaran, A. Iwasa, T. Nawa, T. Sato, K. Kurumisawa, Ion-cement hydrate interactions govern multi-ionic transport model for cementitious materials, Cement Concr. Res. 40 (12) (2010) 1756–1765, https://doi.org/10.1016/j.cemconres.2010.08.019.
[31] H. Zibara, Binding of External Chloride by Cement Pastes, University of Toronto, Canada, 2001 PhD thesis.
[32] B. Guo, Erosion of Chloride in Reinforced Concrete Structures—Migration Mechanism of Multi-Field Coupling and Active Electric Corrosion Control, Harbin Institute of Technology, China, 2018 PhD thesis, (In Chinese).
[33] J. Hu, Y. Wang, Y. Ma, J. Wei, Q. Yu, Identification on acidification damage of external anode system induced by impressed current cathodic protection for reinforced concrete, Math. Biosci. Eng. 6 (16) (2019) 7510–7525.
[34] J. Garcia, F. Almeraya, C. Barrios, C. Gaona, R. Nunez, I. Lopez, M. Rodriguez, A. Martinez-Villafane, J.M. Bastidas, Effect of cathodic protection on steel-concrete bond strength using ion migration measurements, Cement Concr. Compos. 34 (2) (2012) 242–247, https://doi.org/10.1016/j.cemconcomp.2011.09.014.
[35] J. Xu, W. Yao, Current distribution in reinforced concrete cathodic protection system with conductive mortar overlay anode, Construct. Build. Mater. 23 (6) (2009) 2220–2226, https://doi.org/10.1016/j.conbuildmat.2008.12.002.
[36] G.K. Glass, A.M. Hassanein, N.R. Buenfeld, Cathodic protection a orded by an intermittent current applied to reinforced concrete, Corrosion Sci. 43 (2001) 1111–1131.
[37] B. Šavija, J. Pacheco, E. Schlangen, Lattice modeling of chloride diffusion in sound and cracked concrete, Cement Concr. Compos. 42 (2013) 30–40, https://doi.org/10.1016/j.cemconcomp.2013.05.003.